On the Estimation of Mid-Latitude Ionospheric Irregularity Drifts Using a Local Array of GNSS-Based Scintillation Monitors

Isaac G. Wright, Josemaria Gomez Sócola, and Fabiano S. Rodrigues The University of Texas at Dallas

Take-Away: We propose a spaced-receiver framework to estimate ionospheric irregularity drift that combines diffraction-pattern measurements with geometry-based inversion. We demonstrate the proposed method using a local array of three low-cost GNSS-based scintillation monitors (ScintPi 4.0) during a rare mid-latitude scintillation event. The results indicate predominantly westward irregularity zonal motion, poleward-upward meridional motion, and a drift response that has been associated with southward IMF B_z.

1. INTRODUCTION AND MOTIVATION

- Ionospheric irregularities can produce **scintillation**: rapid fluctuations in EM wave amplitude and phase which can negatively impact radio technology.
- Mid-latitude scintillation in **Global Navigation Satellite Systems** (GNSS) signals (L-band: ~1-2 GHz) has been thought to occur much less frequently than scintillation observed at low and high latitudes and is associated only with severe geomagnetic storms (Gomez Socola et al., 2025).
- This idea caused dedicated GNSS scintillation instrumentation to remain sparse at mid-latitudes. As a result, **observations of mid-latitude scintillation have been limited**.
- At the same time, the **spaced-receiver analysis** is a technique which uses time-delayed observations of fluctuations measured by closely spaced receivers to **infer the velocities of the irregularities which produce scintillation.**
  - **Key Limitation:** The measured velocity in the spaced-receiver analysis is a geometry-projected combination of drift components. Its interpretation depends on satellite geometry, array orientation, and assumptions about the irregularity structure and dynamics.

2. MAIN QUESTIONS

Using a new version of low-cost GNSS-based scintillation and TEC monitors (ScintPi 4.0), we deployed **an array of closely-spaced receivers** at the University of Texas at Dallas (UTD) to address science questions including:

Q1: How can the spaced-receiver approach be extended to estimate the perpendicular (zonal and meridional) drift velocity of ionospheric irregularities?

Q2: What can spaced-receiver observations reveal about **mid-latitude irregularity dynamics during the October 2024 geomagnetic storm?**

3. STORM EVENT AND OBSERVATIONS

- The 10–11 October 2024 geomagnetic storm was one of the strongest storms of Solar Cycle 25: Kp ~ 8.7, Dst ~ −346 nT, and IMF Bz < −40 nT.
- During the storm, **intense L-band scintillation** was observed south of the scintillation monitor at UTD (32°N, 96°W; dip latitude ~ 43°).
- The strongest scintillation occurred between 03:00 – 13:00 UTC (~ 20:40–06:40 MLT) on October 11, 2024.
- The timing and location of the scintillation are consistent with irregularities associated with extreme **equatorial plasma bubbles (EPBs)** (Zakharenkova et al., 2025)

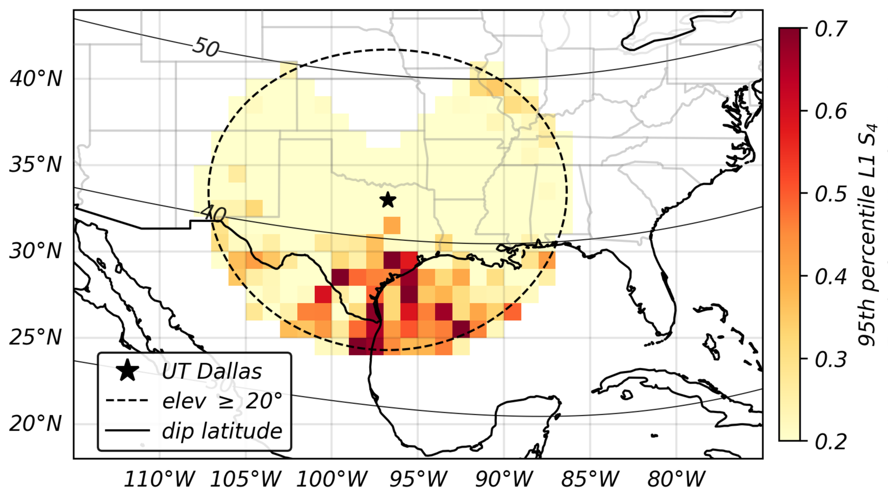

Figure: Amplitude scintillation index (S_4) plot over Texas. S_4 represents the standard deviation of signal intensity normalized by its mean. Colors denote the 95th percentile S_4 value in each 1° bin from 00:00 to 18:00 on October 11, 2024. Calculations assume thin shell at 350 km altitude.

4. INSTRUMENTATION AND ARRAY

- This study uses **ScintPi 4.0** (Wright et al. 2026); the fourth version of a series of low-cost scintillation and Total Electron Content (TEC) monitors (ScintPi) based on off-the-shelf GNSS receivers (Septentrio Mosaic-X5, ~ 700 USD) and Raspberry Pi single-board computers.
- In anticipation of the event, we deployed an **array of three ScintPi 4.0 units** spaced approximately 100 m east-west, 250 m north-south at UTD.
- 50 Hz carrier-to-noise density ratio (C/N0) data are saved to disk and used in post-processing as a proxy for received GNSS signal intensity.

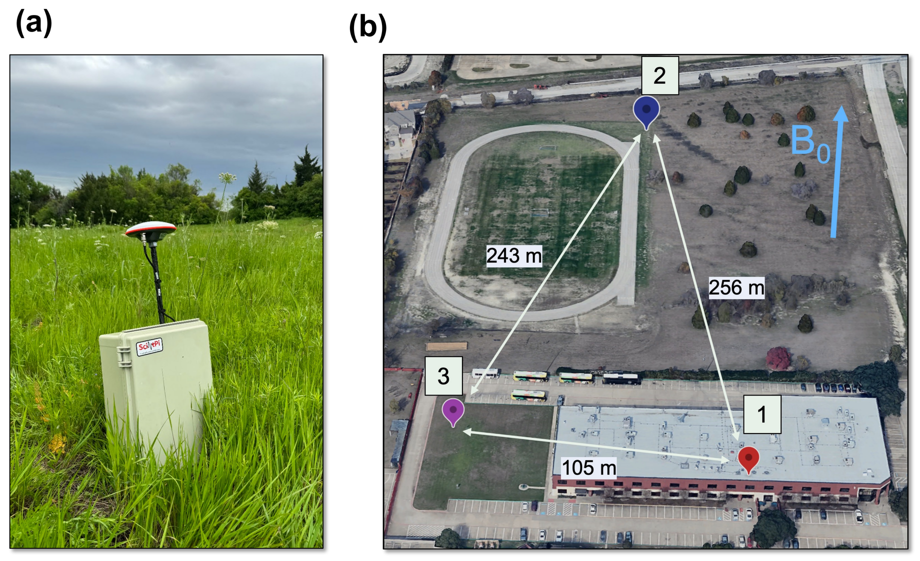

Figure: Experiment array setup: (a) Low-cost GNSS-based scintillation monitor, ScintPi, with antenna and modified portable battery pack design. (b) Google Earth view of the three-station array with local magnetic vector indicated.

5. SPACED-RECEIVER METHOD

Two-Step Approach:

1. Estimating the ground motion of **diffraction patterns** produced by scintillation using signal fluctuations observed from an array of GNSS receivers.
2. Estimating **irregularity drifts** in the ionosphere using the diffraction pattern velocities and geometry-based inversion model.

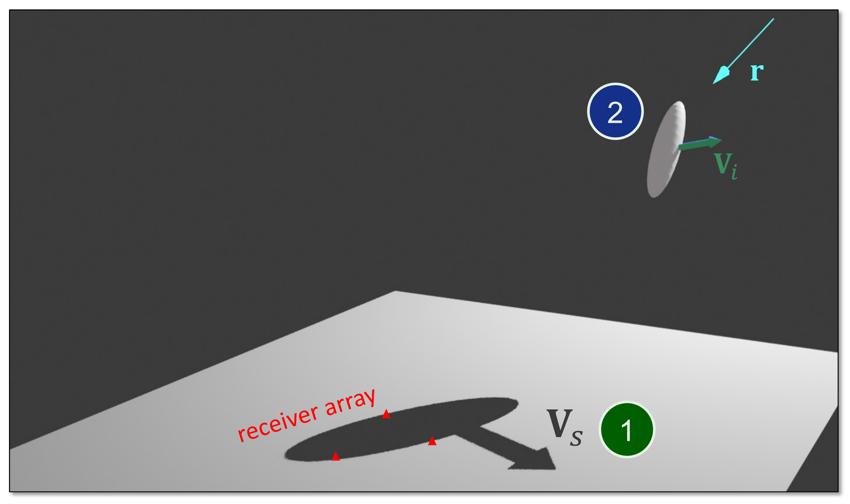

Figure: Schematic of the two-step spaced-receiver method used to infer ionospheric irregularity motion. An ionospheric irregularity drifting with velocity $\mathbf{V}_i$ produces a diffraction pattern whose ground motion, $\mathbf{V}_s$, can be considered a projection of the irregularity motion along the line-of-sight $\mathbf{r}$.

1 Estimating Diffraction Pattern Ground Motion

- Due to elongation of irregularities along B, diffraction patterns are assumed to be **elongated** as well in the diffraction plane.
- Diffraction pattern motion is modeled as the propagation of a plane wave over the receiver array.
- Time delays between receiver pairs are estimated from **cross-correlations of C/N0 fluctuations.**
  - A correction is introduced for time evolution of patterns (Briggs, 1950).
- Magnitude and direction are solved across the three baselines via least squares.
- **Bootstrapping** resampling quantifies statistical uncertainty.

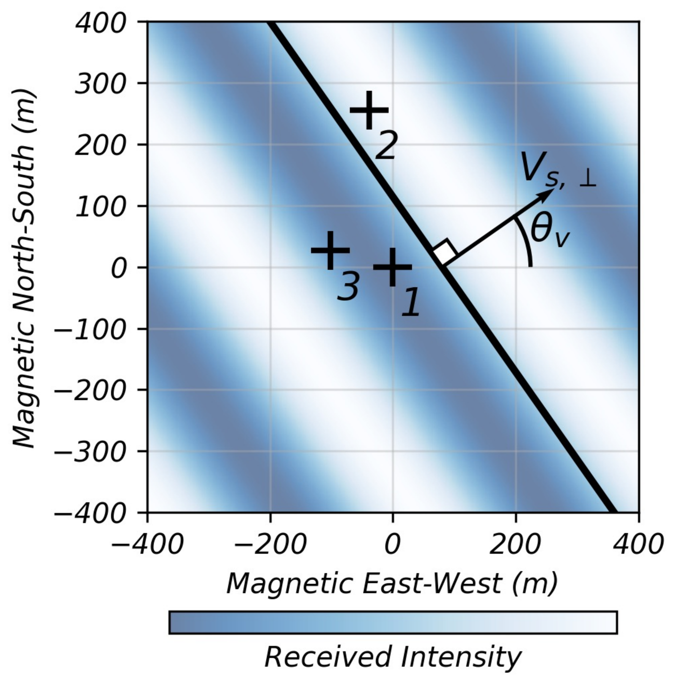

Figure: The ground diffraction pattern is modeled as a plane wave moving with unknown effective velocity $V_{s\perp}$ and direction θ_v across the receiver array.

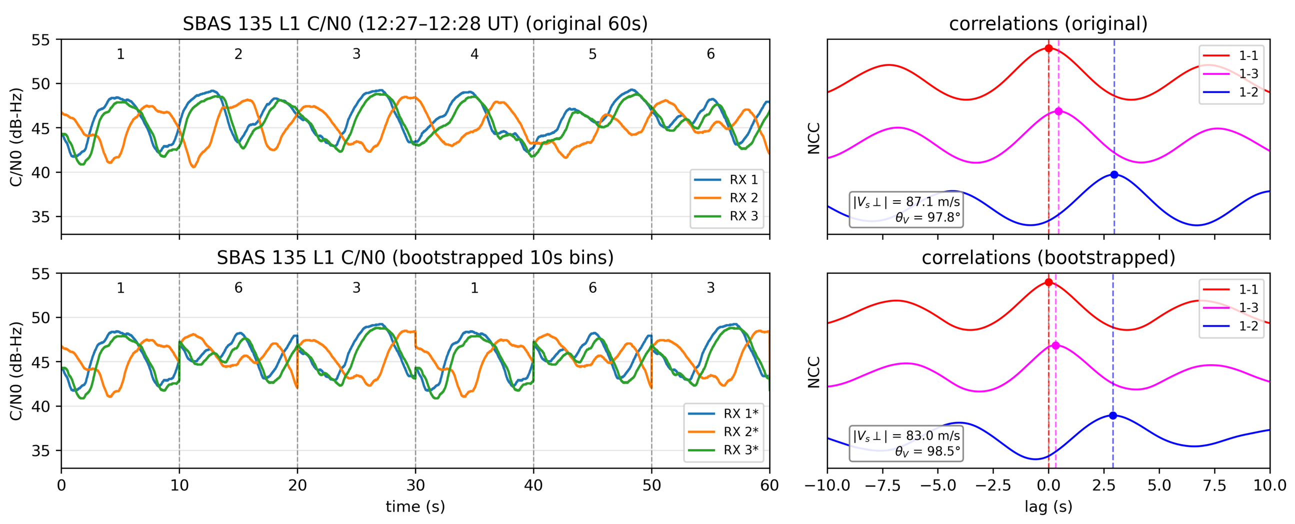

Figure: Illustration of the correlation and bootstrap procedure.
Top: Original C/N0 data (left) and corresponding normalized cross-correlation (NCC) functions (right), shown with peak lags (dashed lines) and the resulting drift estimate.
Bottom: A bootstrap realization created by resampling six 10 s segments with replacement (left) and the recomputed NCC functions (right), yielding a different drift estimate.

2 Estimating Irregularity Drift

Under the assumption of elongated diffraction patterns, the system is effectively projected onto a single transverse direction, **q:**

$$(\mathbf{V}_i + \mathbf{V}_{sat} - \mathbf{V}_s) \cdot \overbrace{(\mathbf{r} \times \mathbf{B})}^{\mathbf{q}} \approx 0$$

Irregularity velocity **(unknown)**; Satellite scan velocity at ionosphere **(known)**; Diffraction pattern velocity **(measured)**; Transverse direction **(known)**

(Ledvina et al., 2004)

- Considering only perpendicular motion, $\mathbf{V}_i$ has **2 unknowns** corresponding to drift components along principal Field Aligned Coordinate (FAC) axes $\hat{x}_{FAC}$ (zonal) and $\hat{z}_{FAC}$ (meridional).
- To close the system, we use **simultaneous GNSS scintillations** observed within an integration window.
- We approximate $\mathbf{V}_i$ as constant between measurements.
- $\mathbf{V}_{sat}$ is estimated from satellite ephemerides; **B** is estimated from IGRF.
- **Integration**: 1-min windows; elevation 15–90°; 90° azimuth span; S_4 > 0.05.
- The estimated velocity, $\hat{\mathbf{V}}_i$, is recomputed using (N = 500) bootstrap realizations to quantify the stability of the solution.

$$\underbrace{\begin{bmatrix} \mathbf{q}_1 \cdot \hat{x}_{FAC} & \mathbf{q}_1 \cdot \hat{z}_{FAC} \\ \mathbf{q}_2 \cdot \hat{x}_{FAC} & \mathbf{q}_2 \cdot \hat{z}_{FAC} \\ \vdots & \vdots \\ \mathbf{q}_N \cdot \hat{x}_{FAC} & \mathbf{q}_N \cdot \hat{z}_{FAC} \end{bmatrix}}_{\mathbf{M}} \underbrace{\begin{bmatrix} \mathbf{V}_{ix} \\ \mathbf{V}_{iz} \end{bmatrix}}_{\hat{\mathbf{V}}_i} = \underbrace{\begin{bmatrix} \mathbf{q}_1 \cdot (\mathbf{V}_{s,1} - \mathbf{V}_{sat,1}) \\ \mathbf{q}_2 \cdot (\mathbf{V}_{s,2} - \mathbf{V}_{sat,2}) \\ \vdots \\ \mathbf{q}_N \cdot (\mathbf{V}_{s,N} - \mathbf{V}_{sat,N}) \end{bmatrix}}_{\mathbf{y}} \qquad \hat{\mathbf{V}}_i = (\mathbf{M}^{\top}\mathbf{M})^{-1}\mathbf{M}^{\top}\mathbf{y}$$

6. VELOCITY ESTIMATION RESULTS

1 Estimating Diffraction Pattern Ground Motion

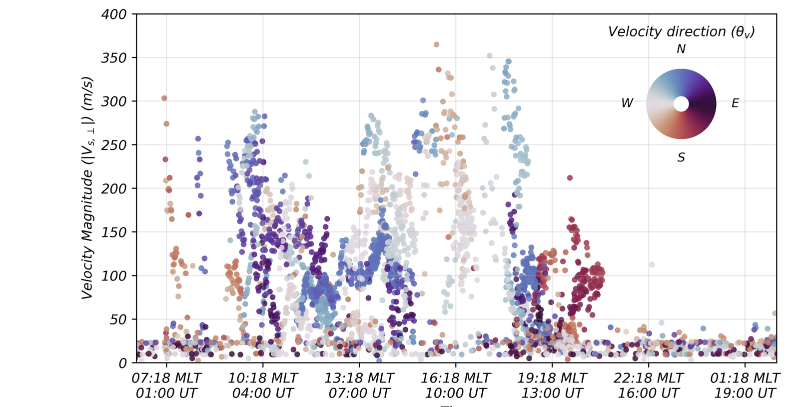

Figure: Diffraction pattern velocities (directions and magnitudes) over time.

- We observed pattern motions with various orientations and averaging 85 m/s in magnitude.
- Here, we point out that the diffraction pattern drift directions and velocities are **difficult to interpret directly.**
- Instead, they depend on **projection geometry** and satellite scanning velocities.

2 Estimating Irregularity Drift

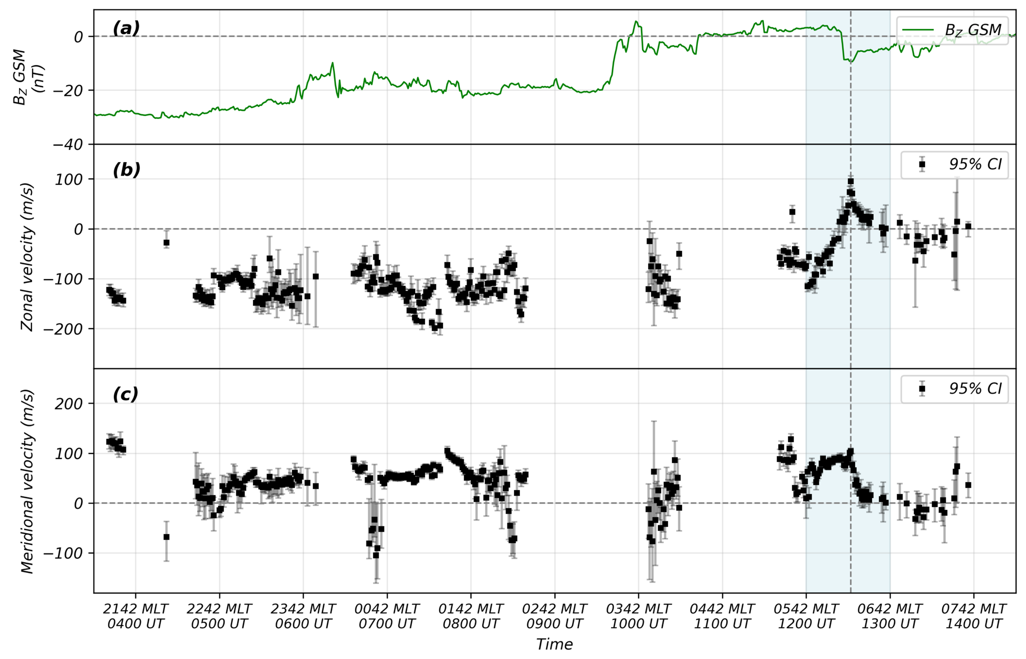

Figure: Irregularity drift estimates during the 11 October 2024 storm. (a) IMF B_z (b) zonal drift and (c) meridional drift. Points show 1-min bootstrap median estimates, with 95% confidence interval error bars. The shaded region and dashed line mark the southward IMF Bz turning near 1230 UT.

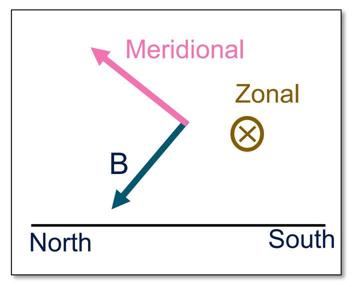

Figure: Sketch of coordinate system. At UTD, **B** is 54° down-ward.

- **Zonal drifts primarily ~ 100 m/s westward,** anomalous compared to quiet night-time EPB drifts which are eastward. This effect is likely associated with storm-time convection potential electric fields.
- **Poleward-upward meridional drifts ~ 50 m/s.**
- Around 12:30 UT, a sudden decrease in the B_z coincides with changes in the zonal and vertical velocities (see Discussions).

7. DISCUSSIONS

Comparisons with Background E×B

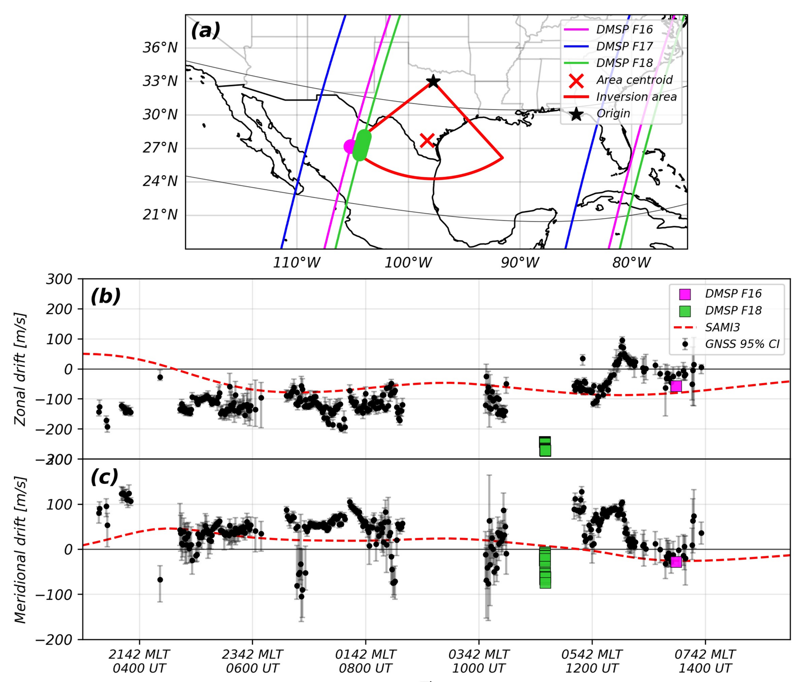

Figure: (a) DMSP ground tracks shown with the inversion region (b) Magnetic zonal drift and (c) magnetic meridional drift estimated from GNSS spaced-receiver scintillation measurements

- GNSS estimates were compared with drifts from SAMI-3 driven by neutral atmosphere model NRLMSIS/HWM (no disturbance dynamo) and Weimer high latitude potential (no prompt penetration) (Huba and Lu, 2024).
- Estimates were also compared with DMSP in-situ ion drifts (~ 850 km altitude).
- Results show **that GNSS drifts are generally consistent with the simulation and satellite data** (westward, poleward-upward).
- However, the exact relationship between background ExB drift and scintillation-derived irregularity drift remains to be determined.

Prompt Penetration Electric Field (PPEF)?

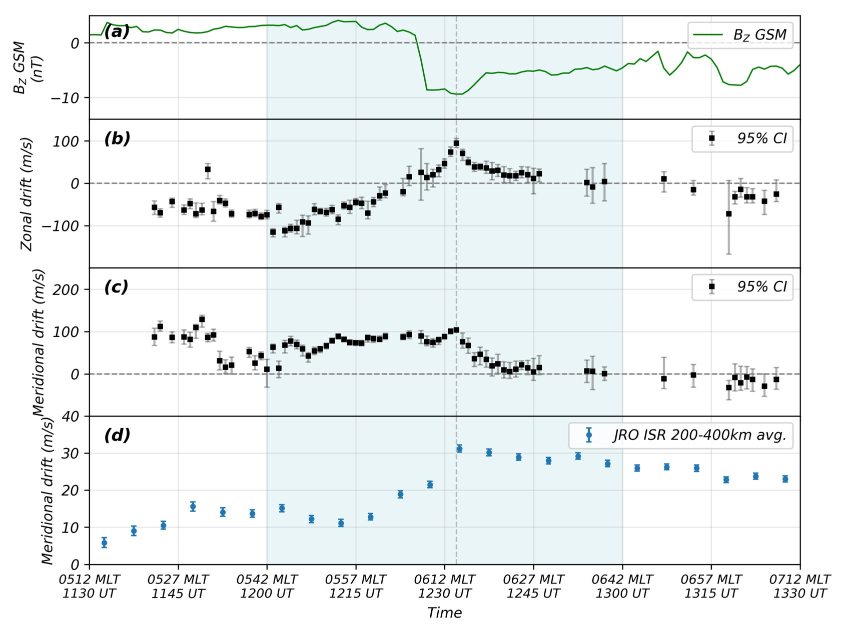

Figure: Zoomed in plot (11:30-13:30 UT) of irregularity drift estimates during the 11 October 2024 storm. (a) IMF B_z, (b) zonal drift, and (c) meridional drift (d) JRO Medium Power meridional (vertical) ISR drifts. The vertical line marks the time of drift estimate change (07:24 MLT at JRO).

- Around 12:29 UT, a **sudden decrease in B_z** from 2nT to -8 nT was followed by **simultaneous increases in the zonal and meridional velocities**, by ~ 50 m/s and 25 m/s (ΔE ~ 2.5 mV/m and 1.3 mV/m, respectively).
- As one possible interpretation, we suggest **prompt penetration of the interplanetary electric field.**
- The timing of ~ 6 minutes between B_z and drift changes is consistent with typical PPEF timescales.
- A dawn-dusk PPEF would be downward at local dawn, producing eastward drifts.
- The drift changes were coincident with an increase of ~ 10 m/s in meridional drifts measured by Jicamarca (JRO) ISR, suggesting global scale.

8. CONCLUSIONS

1. A three-receiver ScintPi 4.0 array captured rare, intense **mid-latitude, L-band scintillation** associated with the 10–11 October 2024 geomagnetic storm.
2. A **new, geometry-based inversion** was used to estimate the motion of the ionospheric irregularities responsible for the observed scintillation (**Q1**).
3. The inversion results show mainly westward and poleward-upward irregularity motion during the storm interval with **strong storm-driven effects** (**Q2**).

THE UNIVERSITY OF TEXAS AT DALLAS

Funding: NSF Graduate Research Fellowship Program under Grant No. 2136516, by NSF Award AGS-2432609, and by the Eugene McDermott Foundation.

Citations: Wright et al (2026) USNC-URSI National Radio Science Meeting (NRSM)
Ledvina et al. (2004), JGR, 109, A10306, doi:10.1029/2004JA010489.
Briggs et al. (1950), Proc. Phys. Soc. B, 63, 106, doi:10.1088/0370-1301/63/2/305.
Zakharenkova et al. (2025), JGR Space Physics, 130, e2025JA033709, doi:10.1029/2025JA033709.
Gomez Socola et al. (2025), Space Weather, 23, e2024SW004213, doi:10.1029/2024SW004213.
Huba and Lu (2024), Geophys. Res. Lett., 51, e2024GL109071, doi:10.1029/2024GL109071.

Contact: igw180000@utdallas.edu